

Appendix F:

Tinker, M.T., D.F. Doak, J.A. Estes, and A.H. Kage. 2004. A spatially explicit simulation model to predict range expansion of the southern sea otter.

This page intentionally left blank.

A SPATIALLY EXPLICIT SIMULATION MODEL TO PREDICT RANGE EXPANSION OF THE SOUTHERN SEA OTTER.

Tinker, M.T., D.F. Doak, J.A. Estes, and A.H. Kage. 2004.

Abstract

1. Reliable projections of future population growth and southward range expansion of the southern sea otter population would be useful for a number of management purposes, and are of interest to several state and federal agencies, including MMS.
2. We developed a spatially explicit simulation model to project population growth and southward range expansion. Our model represents a unique synthesis of a multi-state dispersal matrix with the integrodifference equation approach to calculating invasion speed. The model was parameterized with data from the current study.
3. We used the results of repeated simulations with this model to predict future patterns of range expansion while accounting for uncertainty in model parameters. Although model output closely matched historical data on rates of southward range expansion, simulation results were highly variable, reflecting the uncertainty of estimates of input parameters as well as the uncertainty regarding ultimate causes of variation in survival rates.
4. Males are more likely than females to move long distances, and most of the individuals that travel south of Point Conception are males, yet movement rates of females, particularly those of juvenile and sub-adult females, had much more impact on both population expansion and southward range expansion than those of males.
5. The survival rate of juvenile/sub-adult females in the southern part of the range emerged as a key parameter influencing the rate of range expansion. Fieldwork to improve estimates of this parameter would do much to reduce uncertainty in the model's predictions.
6. Although our model is relatively simple and does not account for many important aspects of sea otter biology and ecology, it makes use of all existing demographic and movement data and provides a robust and generalizable approach to understanding and predicting population dynamics in southern sea otters. This new tool for conservation biologist and managers can be easily expanded and improved as additional data and more precise parameter estimates become available.

Introduction

Data on age- and sex-specific probabilities of survival, reproduction and movement provide the basic tools for understanding past and present population dynamics (Caswell 2001, Doak and Morris 2002), and can also be used for predicting future population dynamics. Such tools are often the basis for conservation and management decisions. In the case of the southern sea otter, developing a realistic projection of future population growth and range expansion at the southern end of the current distribution would facilitate the informed assessment of potential impacts of sea otters on important industries (e.g. fisheries, eco-tourism), potential negative effects of human activity on sea otters (e.g. risks associated with the near-shore transport and extraction of petroleum, entanglement in fishing gear, etc.), and the eventual recovery and de-listing of this threatened species (USFWS 2003). One of the most important outcomes of the current research efforts has been the accumulation of a detailed and extensive database of spatially-explicit demographic and movement information for the southern sea otter. Here, we use these data to develop a spatially structured simulation model for predicting population growth and southward range expansion.

Stage-based projection matrices provide a means of integrating information on population structure, individual survival and reproduction in an intuitive and mathematically useful way. Projection matrices are commonly used to predict future population dynamics, measure the sensitivity of these dynamics to particular vital rates, and elucidate the underlying processes responsible for patterns of interest (Caswell 2001). Multi-state projection matrices represent an extension of the basic matrix approach, and can be utilized when population structure or environmental conditions vary with geographic location, or when the effects of individual movements between sub-populations are thought to be important (Lebreton and Gonzalez-Davila 1993). Multi-state projection models facilitate the quantitative interpretation of source-sink dynamics (e.g. Doak 1995), and can help to clarify the relative importance of survival and dispersal in driving population trends (e.g. Lebreton and Gonzalez-Davila 1993).

Multi-state matrices are often used to study metapopulation dynamics and the colonization rate of unoccupied habitat (Caswell 2001). The latter phenomenon can also

be modeled as a continuous variable using integrodifference equations, as described by Neubert and Caswell (2000). This relatively new technique utilizes stage-specific data on dispersal and vital rates to derive the asymptotic speed at which the population front (or “traveling wave”) will invade empty habitat (Neubert and Caswell 2000). Note that for the purpose of our analyses we will define the term “dispersal” in a purely quantitative, descriptive sense, referring to the average linear distance moved (or mean net displacement) between the location of an individual at time $t=1$ and the location at $t=2$. This definition makes no reference to the biological cause or behavioral significance of the movements, which may often differ between age and sex classes.

In the case of the southern sea otter, analyses of multiple data sets indicate that demographic rates are not constant across the sea otters range, but vary between broad geographic areas (Figure 1; Chapter 2, this report). Moreover, it appears that individual dispersal distances also vary by age and sex class (Chapter 3, this report). A multi-state projection matrix model would therefore be an appropriate tool for elucidating the relative importance of dispersal and survival in driving population dynamics at the range peripheries. The interaction between stage-specific dispersal and vital rates will also likely determine the rate and pattern of population expansion into unoccupied territory, a phenomenon best described using integrodifference equation models (Neubert and Caswell 2000). We couple these two techniques in a spatially explicit simulation model, parameterized using data from the current study (Chapter 2, this report), and use the results of repeated simulations to predict future patterns of range expansion while accounting for uncertainty in model parameters. We then use sensitivity analysis to determine the relative importance of each model parameter, in order to highlight specific areas where further study will be particularly useful.

Methods

Matrix Structure

A stage-based, 2-sex projection matrix (Caswell 2001) was used to describe annual transitions between 4 age-classes: juveniles (defined as 1 year post-weaning), sub-adults (2 and 3-year-olds), prime-age adults (4–10-year-olds) and aged adults (11 years of age or older). Specifically, we constructed an 8×8 matrix of the form:

$$\mathbf{A} = \begin{array}{c} \begin{array}{cc} & \begin{array}{cccc} \text{Sex} = \text{f} & & & \end{array} & \begin{array}{cccc} \text{Sex} = \text{m} & & & \end{array} \\ \begin{array}{c} \text{Sex} = \text{f} \\ \\ \\ \end{array} & \begin{array}{cccc|cccc} 0 & R_{1,2} & R_{1,3} & R_{1,4} & 0 & 0 & 0 & 0 \\ G_{2,1} & P_{2,2} & 0 & 0 & 0 & 0 & 0 & 0 \\ 0 & G_{3,2} & P_{3,3} & 0 & 0 & 0 & 0 & 0 \\ 0 & 0 & G_{4,3} & P_{4,4} & 0 & 0 & 0 & 0 \end{array} \\ \hline \begin{array}{c} \text{Sex} = \text{m} \\ \\ \\ \end{array} & \begin{array}{cccc|cccc} 0 & R_{5,2} & R_{5,3} & R_{5,4} & 0 & 0 & 0 & 0 \\ 0 & 0 & 0 & 0 & G_{6,5} & P_{6,6} & 0 & 0 \\ 0 & 0 & 0 & 0 & 0 & G_{7,6} & P_{7,7} & 0 \\ 0 & 0 & 0 & 0 & 0 & 0 & G_{8,7} & P_{8,8} \end{array} \end{array} \quad 1$$

where each element of \mathbf{A} , $a_{j,i}$, represents the transition from age/sex class i to age/sex class j . Note that $i \leq 4$ correspond to female age-classes, while $i \geq 5$ correspond to male age classes. Three types of transition are identified in \mathbf{A} : G , P and R . The first type of transition, G , represents survival and growth: in other words, the probability that individuals survive for 1 year and advance to the next age-class. The second type, P , represents “persistence”, or survival without transition to the next age class. The final type of transition, R , represents survival and successful reproduction: for our purposes, an individual female is considered to have successfully reproduced if she gives birth and successfully weans a pup (i.e. she contributes a single viable juvenile to the population).

To estimate P , G and R we used standard equations for deriving fixed-stage-duration transition probabilities from underlying vital rates (Caswell 2001):

$$P_{i,i} = s_i \cdot \left(1 - \frac{(s_i/\lambda)^{T_i} - (s_i/\lambda)^{T_i-1}}{(s_i/\lambda)^{T_i} - 1} \right) \quad 2$$

$$G_{j,i} = s_i \cdot \left(\frac{(s_i/\lambda)^{T_i} - (s_i/\lambda)^{T_i-1}}{(s_i/\lambda)^{T_i} - 1} \right) \quad 3$$

$$R_{j,i} = s_i \cdot \frac{1}{2} b_i \cdot w_i \quad 4$$

where T_i is the stage duration (in years) for age/sex class i , λ is the annual rate of population growth, s_i is the annual survival rate for an individual of stage i , b_i represents the birth rate for a female of stage i and w_i represents the weaning success rate for a female of stage i . We assumed a 1:1 sex ratio at birth.

Matrix **A** was used to model the basic demographic processes for sea otters at a particular time and place. The next step was to introduce spatial structure to the model by constructing a multi-state matrix. Consider a structured population consisting of three sub-populations, each of which exhibits unique demographic properties, and between which there is no potential for dispersal. A multi-state matrix for such a population would be:

$$\mathbf{B} = \begin{matrix} & \begin{matrix} A_{1,1} & 0 & 0 \end{matrix} \\ \begin{matrix} 0 & A_{2,2} & 0 \\ 0 & 0 & A_{3,3} \end{matrix} & \end{matrix} \quad 5$$

where each cell of matrix **B** represents a transition from sub-population x to sub-population y . The diagonal of **B** consists of sub-matrices $\mathbf{A}_{y,x}$ (where $y = x$), each of which describes demographic processes for a single sub-population according to equation 1. All other elements of **B** are set to 0 because we specified no dispersal between sub-populations.

Unfortunately, although equation 5 is conceptually very simple, it is also unrealistic: for more realistic dynamics we must allow dispersal between sub-populations. Accordingly, let $m_{i,x \rightarrow y}$ represent the probability of moving to sub-population y for an individual of stage i that starts the year in sub-population x . These probabilities can be incorporated into a new matrix, **M**, that has a general structure identical to **A** but whose elements correspond to stage-specific dispersal probabilities ($m_{i,x \rightarrow y}$) rather than survival or reproduction. Dispersal probabilities between sub-populations can be calculated from empirically-derived dispersal distance distributions. We assumed that the annual dispersal distance for an individual sea otter of stage i at location x' (i.e. somewhere within sup-population x) could be described by a Laplace probability distribution with shape parameter $\sigma_{i,x}$. The Laplace distribution essentially

consists of two back-to-back exponential distributions, and was considered appropriate for modeling sea otter movements in California because animals are restricted to dispersal in one of two directions (north or south along the coast).

We defined each sub-population spatially by its northern and southern boundaries along the ATOS line (the “as the otter swims” line, corresponding to a series of points at 500m increments, north to south, along the 10m bathymetric contour); thus sub-population y was spatially defined by boundary points y_N and y_S , and spanned $0.5(y_S - y_N)$ km of coastline. The probability that an individual located at point x' would disperse to sub-population y was estimated as the absolute difference between the Laplace cumulative distribution function evaluated at values $y_N - x'$ and $y_S - x'$:

$$m_{i(x') \rightarrow y} = \left| \left(1 - \frac{1}{2} \exp\left(\frac{y_N - x'}{\sigma_{i,x}} \right) \right) - \left(1 - \frac{1}{2} \exp\left(\frac{y_S - x'}{\sigma_{i,x}} \right) \right) \right| \quad 6$$

and the net probability of dispersal from sub-population x to sub-population y was estimated as:

$$m_{i,x \rightarrow y} = \sum_{x'=x_N}^{x_S} (m_{i(x') \rightarrow y}) p(x') \quad 7$$

where $p(x')$ sums to 1 for $x_N \leq x' \leq x_S$ and represents the probability that an individual animal from sub-population x would be located at x' . For simplicity we used discrete summation, rather than continuous integration, thereby assuming that all points within a 500m interval (or ATOS unit) would be adequately represented by a single integer value of x' . A uniform spatial distribution of individuals within each sub-population would have allowed us to define $p(x') = 1/(x_S - x_N + 1)$; however, examination of annual range-wide survey counts suggested that sea otters were not uniformly distributed but were often skewed towards one boundary or clumped within one region. To account for this non-uniformity, we used beta probability functions to represent the spatial distribution of otters within each sub-population. Specifically, we fit beta distributions to the raw survey data for each sub-population (using data from the 5 most recent spring counts; Figure 2), having first standardized the location data to values between 0 and 1 (where 0 corresponded to the northern boundary and 1 corresponded to the southern boundary of

the sub-population). Using the resulting beta functions we could then calculate the probability that an individual from sub-population x would be located at x' :

$$p(x') = \beta\left(a, b, \frac{x' - x_N + 1}{x_N - x_S + 1}\right) - \beta\left(a, b, \frac{x' - x_N}{x_N - x_S + 1}\right) \quad 8$$

where $\beta(a, b, Z)$ represents the beta cumulative distribution function with parameters a and b , evaluated at value $= Z$.

Equations 6 – 8 were solved for each pair of sub-populations, including the special case when $y = x$ (which corresponds to the probability of remaining within the same sub-population). To ensure that $\sum m_{i,x \rightarrow y} = 1$ for each combination of i and x , we made the simplifying assumption that individuals whose dispersal distance brought them to the range end would “bounce off” this boundary. This was accomplished by a minor adjustment to equation 6 when the target sub-population was a range end: when the target was the northern-most end of the range, $y_N - x'$ was set to ∞ , and when the target was the southern-most end of the range, $y_S - x'$ was set to ∞ .

Combining the two types of matrix, \mathbf{M} and \mathbf{A} , we constructed a multi-state matrix which allowed for movements between sub-populations (illustrated again with just three sub-populations for simplicity):

$$\mathbf{B} = \begin{matrix} & \begin{matrix} A_{1,1} \circ M_{1,1} & A_{1,2} \circ M_{1,2} & A_{1,3} \circ M_{1,3} \end{matrix} \\ \begin{matrix} A_{2,1} \circ M_{2,1} & A_{2,2} \circ M_{2,2} & A_{2,3} \circ M_{2,3} \end{matrix} & & \\ \begin{matrix} A_{3,1} \circ M_{3,1} & A_{3,2} \circ M_{3,2} & A_{3,3} \circ M_{3,3} \end{matrix} & & \end{matrix} \quad 9$$

Each cell of matrix \mathbf{B} consists of the Hadamard product of a demographic matrix and a movement matrix ($\mathbf{A}_{y,x} \circ \mathbf{M}_{y,x}$, where \circ represents element-by-element multiplication). The resulting elements of each sub-matrix therefore represent joint probabilities of moving from x to y and then successfully making the transition from stage i to stage j . Note that the diagonal of \mathbf{B} is mathematically identical to all other cells, though it actually represents the special case where individuals do not disperse. For computational simplicity we required that individuals disperse at the start of each new year, after which survival, growth and reproduction occur at the new location: this results in a demographic sub-matrix $\mathbf{A}_{y,x}$ that is identical for all cells in a given row of \mathbf{B} .

Simulating Range Expansion

The multi-state matrix model in equation 9 accounts for dispersal and demographic processes within the existing range of the southern sea otter at time t . It does not, however, account for the expansion of the existing range boundaries to the north and south. In order to predict the expansion of the population into un-occupied territory, we developed an integrodifference equation model (Neubert and Caswell 2000). This approach utilizes a stage-based demographic matrix, in conjunction with the moment generating functions of stage-specific dispersal kernels (in this case, the Laplace distribution functions described above) to solve for the asymptotic speed of the “traveling wave” formed by the population front as it moves into empty habitat. The asymptotic wave speed has been found to correspond well to the rate of population range expansion in both numerical simulations and empirical data sets (Neubert and Caswell 2000); we therefore used it to estimate the rate at which the range boundaries of the sea otter population will move to the south and north over time.

To predict southward range expansion, we populated demographic matrix \mathbf{A} with vital rates corresponding to the southern-most sub-population, and used this in conjunction with the appropriate Laplace distribution parameters to solve the integrodifference equation for the asymptotic wave speed, following the methods outlined by Neubert and Caswell (2000). We used the same approach to predict northward range expansion, using vital rates and dispersal kernels corresponding to the northern-most sub-population. The resulting estimates of range expansion speed were used to re-set the northern-most and southern-most sub-population boundaries on an annual basis; this of course had the effect of altering the predicted rates of dispersal to and from these sub-populations, and so equations 6 through 9 were re-solved after each year of population projection.

Model Parameterization

The results of maximum likelihood analyses of mark-recapture data and 10 years of carcass age structure data (see Chapter 2) suggest that the southern sea otter population consists of 4 sub-populations, identified based on consistent differences in vital rates: these correspond to the northern, north-central, south-central and southern portions of the current sea otter range (Figure 1). We identify 2 additional areas for the purpose of this

simulation: these are the population “frontal” areas, defined as recently-occupied areas at the northern and southern ends of the range that are currently utilized seasonally and exclusively by males (each frontal area spans 30 km of coastline; Figure 1). The resulting 6 sub-populations were defined spatially as follows:

1. Northern front, North of Pigeon Pt. (ATOS 90–149)
2. Northern periphery, Pigeon Pt. – Santa Cruz (ATOS 150–230)
3. North-central, Santa Cruz – Pt. Sur (ATOS 231–500)
4. South-central, Pt. Sur – Pt. Buchon (ATOS 501–844)
5. Southern periphery, Pt. Buchon – Pt. Conception (ATOS 845–1110)
6. Southern front, South of Pt. Conception (ATOS 1111–1170)

Note that the ATOS outer boundaries for 1 and 6 correspond to the current range limits (2003–2004), and were used to initiate forward simulations. We define the southern and northern range boundaries as the two points on the ATOS line spanning 99.5% of the spring survey count (allowing for up to 4 outlying individual animals at each end), recognizing that this is somewhat arbitrary and that some animals will occasionally be observed well beyond these boundaries. Also, we assumed that sea otters in the frontal areas would exhibit identical vital rates to those in the neighboring sub-populations (although the age/sex structure would be different). Thus vital rates from sub-population 2 were used to parameterize 1, and vital rates from 5 were used to parameterize 6.

To account for uncertainty associated with future population dynamics we used a re-sampling approach, utilizing the range of available vital rate estimates to parameterize the demographic matrices uniquely for each new simulation. Analyses of carcass age structure data provided 10 years (1992–2001) of estimates for each sub-population (Chapter 2). Mark-recapture analyses of telemetry provided two more sets of estimates, one for the 1980’s (Siniff and Ralls 1988, Siniff and Ralls 1991) and one for 2001–2003 (Chapter 2). Accumulating evidence suggests that there has been very little variation in reproduction parameters over the past 20 years, so we used a single set of age-specific rates for all simulations: these were set according to the birth rates and weaning success rates calculated from radio-tagged study animals at San Simeon (Chapter 2) and were also consistent with values reported in the literature (Siniff and Ralls 1991, Jameson and

Johnson 1993, Riedman et al. 1994). All of the estimates for demographic parameters that we used for simulations are summarized in Table 1.

Movement probabilities were parameterized by fitting Laplace probability distributions to annual dispersal distances that had been recorded from radio-tagged study animals (Figure 3). Raw data were available for 72 study animals from the current study, with movements restricted primarily to the south half of the range; these data were augmented by data from a concurrent study in the north half of the range (Bodkin and Staedler, unpublished data) and from a similar telemetry study in the 1980's (Siniff and Ralls 1988, Ralls et al. 1996). Further details about the collection and analyses of movement data can be found in Chapter 3. For this particular analysis we used maximum likelihood methods to fit probability distributions for 4 age/sex classes: juvenile/sub-adult females, adult females, juvenile/sub-adult males and adult males. The juvenile/sub-adult age classes and adult/aged-adult age classes were pooled because there were insufficient sample sizes (particularly for juveniles) to allow calculation of separate distributions. Dispersal distance kernels were calculated separately for the north half and south half of the range, and for the southern range front in the case of males. Preliminary analysis indicated that only the data for adult males differed significantly between sub-populations, and so data were pooled across areas for the other age/sex classes. For each probability distribution we calculated the 95% confidence intervals around $\sigma_{i,x}$ (Table 1), and used this range of values to parameterize movement matrices and dispersal kernel functions.

Running Simulations

Projecting population dynamics can be accomplished simply by matrix multiplication with a population vector. The population vector consists of the number of animals in each stage-class, thus the vector length must equal the number of rows in the projection matrix: in this case, 8 values (4 stages for each sex) for each sub-population, giving a total length of 48. One common way to initialize such a population vector is to multiply an estimate of population size (in this case the survey count for 2003) by the stable stage distribution (SSD) calculated from the matrix using standard algebraic techniques (Caswell 2001). However, this approach requires the assumption that demographic rates have been approximately stable for long enough that the age

distribution has converged on the SSD: in the case of the southern sea otter, there is considerable evidence that this has not been the case (Estes et al. 2003a). Consequently, prior to running forward simulations (i.e. to project future population growth and range expansion), it was necessary to run a historical or “hind-cast” simulation to initialize the age-structure for each sub-population. To accomplish this, we utilized the historical demographic rates presented in Table 1 to simulate population dynamics from 1989 to 2003.

We initialized the 1989 population vectors for each sub-population by multiplying the 1989 spring census count by the SSD associated with the 1980’s demographic rates (Table 1, estimate 12). Movement matrices were parameterized using the best-fit dispersal kernels for each age/sex class. We then projected 14 years of population dynamics (Figure 4), calculating all demographic transitions, dispersal and range expansion rates as explained above. We adjusted the demographic rates for the 4th–14th years of the projection (1992 to 2003), setting them to equal the appropriate maximum likelihood estimates (Chapter 2; Table 1, estimates 1–11). The outcome of this historical projection was an expected population vector for 2003, which was used to initialize stage distributions for all forward simulations. An additional result was a comparison of expected vs. observed population counts and expected vs. observed range expansion, which we used as a way of graphically evaluating the efficacy of our model structure, assumptions and parameter values.

We conducted forward simulations in a similar way, projecting 15 years of population dynamics and range expansion using matrix multiplication. We first created 500 unique dispersal kernels by randomly selecting stage- and location-specific Laplace distribution parameters ($\sigma_{i,x}$) from within the ranges listed in Table 1. For each of the resulting 500 movement matrices, we ran 20 simulations using different demographic matrices: the first 10 iterations were parameterized using the best-fit maximum likelihood values from 1992–2001 (Chapter 2; Table 1, estimates 1–10), while for iterations 11–20 we randomly selected vital rates from within the 80% confidence intervals associated with mark-recapture parameter estimates (Chapter 2; Table 1, estimates 10–11). Confidence intervals for each estimate were calculated from standard errors using a logit-based “back transform” method (Burnham and Anderson 1998). The random

combinations of dispersal and demographic estimates resulted in 10,000 unique iterations of the simulation model.

We summarized simulation results graphically by plotting frequency histograms of three key results: the predicted number of independent otters south of Pt. Conception (i.e. in sub-population 6) after 10 years, the predicted number after 15 years, and the predicted rate of range expansion to the south (in units of km/year). We estimated the mean, median, mode and variance for these three variables, as well as their 95% confidence limits. To calculate confidence intervals we assumed a negative binomial probability distribution in the case of the number of otters south of Pt. Conception, and a Weibull probability distribution in the case of the range expansion speed. We also estimated summary statistics for the net population growth rate (λ , calculated as the geometric mean rate of growth for each simulation), which was normally distributed.

Finally, we calculated the sensitivity of simulation results to all model parameters using multiple regression analysis: specifically, we calculated the proportion of variance in three response variables (the predicted number of otters south of Pt. Conception after 15 years, the rate of southward range expansion, and λ) explained by each of the demographic and dispersal parameters, after accounting for variance due to all other parameters. Individual variance components were estimated by their partial coefficients of determination (r^2_p), following (Neter et al. 1990).

Results

The historical projection simulation resulted in population dynamics that were consistent with observed survey counts over the same period (Figure 4a). While this was not especially surprising (the survey counts were one of the data sets used to fit the demographic rates, along with carcass data), it nonetheless suggested that the resulting stage distribution vector for 2003 was reasonably accurate, and also clearly demonstrates the range of different growth rates possible under the simulation parameters. Also encouraging was the close agreement between actual southward range expansion over the past 15 years and the predicted population wave speed. Although the position of the southern range boundary from year-to-year was highly variable, the long-term trend was fit by a linear expansion rate of approximately 4.9 km/year ($R^2 = 0.59$). The mean predicted rate of expansion over the same period, as calculated from stage-specific dispersal and demographic rates, was 3.95, a value not significantly different from the observed trend (Figure 4b).

The net annual rate of population increase (λ) for all forward simulations was 1.01, and 95% of the simulations resulted in λ of 0.971–1.052. The rate of population growth to the south of Pt. Conception surpassed that of the rest of the population in almost all instances, with 95% of the simulations showing a rate of increase south of Pt. Conception of 4–20% per year. The median number of independent otters south of Pt. Conception after 10 years was 117, and after 15 years this value had increased to 131 (Figure 5). The rapid growth to the south was partly attributable to dispersal from other portions of the population, but also reflected a high intrinsic rate of growth. The interaction between dispersal and intrinsic population increase resulted in continued range expansion to the south in virtually all simulations: the median predicted wave speed was 4.9 km/year over the 15 year projection (Figure 6). Interestingly, this wave speed is precisely the same as the average rate of expansion over the past 15 years (Figure 4). Continued range expansion at this median rate would mean that after 10 years the southern range boundary will have moved to a location near Santa Barbara harbor mouth (ATOS = 1267), and after 15 years to Carpinteria (ATOS = 1316). There is a great deal

of uncertainty around these estimates: the 95% confidence interval for the 15 year estimate was $ATOS = 1183-1584$. Table 2 summarizes all simulation statistics.

The simulation results were sensitive to both variation in dispersal and variation in survival parameters, but the relative magnitude of sensitivities was quite different for different response variables. Variation in dispersal parameters had the most substantial impact on the predicted number of individuals south of Pt. Conception, but had a negligible effect on net population growth (Figure 7). Not surprisingly, variation in survival rate parameters at the south end of the range had a strong effect on all three response variables; however, while variation in survival rates at the center of the range had minimal effect on future range expansion and population growth south of Pt. Conception, their impact on net population growth was three times greater than survival rates at the south end of the range (Figure 7).

A closer inspection of stage-specific sensitivities showed that, in terms of dispersal, juvenile/sub-adult female movement rates had the greatest effect on population growth and range expansion to the south (Figure 8). Dispersal of Juvenile/Sub-adult males had a significant effect on the expected number of individuals south of Pt. Conception, but virtually no effect on the rate of southward range expansion. Adult male dispersal had almost no effect on the simulation results, despite the long-distance movements frequently conducted by this class of animals. Stage-specific survival rates showed a similar pattern of sensitivities: variation in sub-adult female survival had the greatest impact on simulation results, while juvenile and adult female survival had less of an effect (Figure 9). The only result showing any sensitivity to male survival rates was the number of otters south of Pt. Conception, and variation in male survival had almost no effect on the rate of range expansion or on net population growth.

Discussion

The predictions of our hind-cast model closely matched the historical data on rates of southward range expansion, suggesting that estimation of asymptotic wave speed (Neubert and Caswell 2000) is an appropriate technique for simulating range expansion of southern sea otters. This method is particularly appropriate for a population that is expanding along a 1-dimensional axis, as is the case with the southern sea otter. Because it incorporates information on stage-specific dispersal probabilities, demographic rates and population structure, the integrodifference approach is also likely to provide a better approximation to range expansion dynamics than the 1-dimensional diffusion model used previously to model invasion speed in sea otters (Lubina and Levin 1988).

Explicit analysis of uncertainty can provide useful insights to managers (Doak and Mills 1994, Pascual and Adkison 1994, Ralls and Taylor 2000). The best way to incorporate uncertainty into management decisions is to consider, as in our analysis, the full range of expected outcomes (Gerber et al. *in press*). Projections of both the number of independent otters at Point Conception and the rate of southward range expansion were highly variable, reflecting the uncertainty in input parameter estimates and uncertainty about the ultimate causes of fluctuations in survival rates, such as density dependence, disease, and fishing interactions.

Despite this variability, sensitivity analysis of the model's predictions gave us a greatly improved understanding of the processes underlying population growth and range expansion. Sensitivity analysis in this case serves two main purposes. First, it identifies the parameters to which the model is most sensitive: better estimates of these parameters will therefore do most to improve the precision of the model predictions. Our analysis identified the survival rate of juvenile and sub-adult females at the end of range as a key parameter influencing both population growth and range expansion to the south of Pt. Conception. Hence, fieldwork designed to improve estimates of survival rates of young females in southern areas would do most to reduce uncertainty in these particular predictions.

Second, sensitivity analysis highlights the particular components of the population that are driving range expansion and/or population growth. These results are sometimes

not intuitively obvious. For example, although males are more likely to move long distances than females and most of the individuals that travel south of Point Conception are males, male movements proved much less important than female movements (Figure 8). Movement rates of juvenile and sub-adult females had the greatest effect on both population growth and range expansion to south, whereas dispersal of their male counterparts had no impact on the rate of southward range expansion, and variation in adult male survival had almost no effect on either population growth or range expansion. This last result is not so surprising considering that range expansion by males alone would provide no intrinsic population growth (i.e. reproduction) at the ends of the range: because reproduction is ultimately what drives population growth and subsequent range expansion, it is the movement and survival of females that is the limiting factor for both processes. This method of sensitivity analysis also allows for evaluation of spatial patterns: for instance, female survival at the center of the range probably has little effect on the rate of range expansion, but is the most important demographic parameter for predicting growth of the population as a whole (Figure 7).

Our simple multi-state matrix model does not explicitly account for a variety of important aspects of sea otter biology and ecology: these include density dependence (Laidre et al. 2001), spatial and temporal variation in habitat quality (Doak 1995, Thomas and Kunin 1999, Virgl and Messier 2000), responses to ephemeral phenomenon such as episodic prey recruitment events (Watt et al. 2000), seasonal reproductive peaks and movement patterns (Jameson 1989), and important behavioral characteristics such as dietary specializations (Estes et al. 2003b), territoriality (Jameson 1989), contagious distribution, and male/female (or age class) segregation at smaller spatial scales. It is worth noting that the model actually does implicitly account for some of these factors (such as density dependence and habitat quality), in so far as these factors have affected past and present vital rates and movement probabilities within the existing range.

Despite the above-mentioned limitations, our model provides a robust and generalizable approach to understanding and predicting population dynamics in southern sea otters by making use of all existing demographic and dispersal data. It represents a unique synthesis of a multi-state dispersal matrix and the integrodifference equation approach to calculating invasion speed. Our model should provide a useful and flexible

tool for conservation biologists and managers, and can be easily expanded upon or improved as additional data and more precise parameter estimates for southern sea otters become available.

References

- Burnham, K. P., and D. R. Anderson. 1998. Model selection and inference: a practical information-theoretic approach, 2nd edition. Springer-Verlag, New York, NY.
- Caswell, H. 2001. Matrix population models: construction, analysis, and interpretation, 2nd ed edition. Sinauer Associates, Sunderland, MA.
- Doak, D. F. 1995. Source-sink models and the problem of habitat degradation: general models and applications to the Yellowstone grizzly. *Conservation Biology* 9:1370-1379.
- Doak, D. F., and L. S. Mills. 1994. A useful role for theory in conservation. *Ecology* 75:615-626.
- Doak, D. F., and W. F. Morris. 2002. Quantitative conservation biology: theory and practice of population viability analysis. Sinauer Associates, Sunderland, MA.
- Estes, J. A., B. B. Hatfield, K. Ralls, and J. Ames. 2003a. Causes of mortality in California sea otters during periods of population growth and decline. *Marine Mammal Science* 19:198-216.
- Estes, J. A., M. L. Riedman, M. M. Staedler, M. T. Tinker, and B. E. Lyon. 2003b. Individual variation in prey selection by sea otters: Patterns, causes and implications. *Journal of Animal Ecology* 72:144-155.
- Gerber, L. R., T. Tinker, D. Doak, and J. Estes. in press. Mortality sensitivity in life-stage simulation analysis: A case study of southern sea otters. *Ecological Applications*.
- Jameson, R. J. 1989. Movements, home range, and territories of male sea otters off central California. *Marine Mammal Science* 5:159-172.
- Jameson, R. J., and A. M. Johnson. 1993. Reproductive characteristics of female sea otters. *Marine Mammal Science* 9:156-167.
- Laidre, K. L., R. J. Jameson, and D. P. DeMaster. 2001. An estimation of carrying capacity for sea otters along the California coast. *Marine Mammal Science* 17:294-309.
- Lebreton, J. D., and G. Gonzalez-Davila. 1993. An introduction to models of subdivided populations. *Journal of Biological Systems* 1:389-423.
- Lubina, J. A., and S. A. Levin. 1988. The spread of a reinvading species: Range expansion in the California sea otter. *American Naturalist* 131:526-543.

- Neter, J., W. Wasserman, and M. H. Kutner. 1990. Applied linear statistical models: Regression, analysis of variance, and experimental designs, 3rd edition. Irwin, Chicago, IL.
- Neubert, M. G., and H. Caswell. 2000. Demography and dispersal: Calculation and sensitivity analysis of invasion speed for structured populations. *Ecology* 81:1613-1628.
- Pascual, M. A., and M. D. Adkison. 1994. The decline of the Steller sea lion in the northeast Pacific: demography, harvest or environment? *Ecological Applications* 4:393-403.
- Ralls, K., T. C. Eagle, and D. B. Siniff. 1996. Movement and spatial use patterns of California sea otters. *Canadian Journal of Zoology* 74:1841-1849.
- Ralls, K., and B. L. Taylor. 2000. Better policy and management decisions through explicit analysis of uncertainty: new approaches from marine conservation biology. *Conservation Biology* 14:1240-1242.
- Riedman, M. L., J. A. Estes, M. M. Staedler, A. A. Giles, and D. R. Carlson. 1994. Breeding patterns and reproductive success of California sea otters. *Journal of Wildlife Management* 58:391-399.
- Siniff, D. B., and K. Ralls. 1988. Population status of California sea otters: MMS 14-12-001-30033. U.S. Department of Interior, Minerals Management Service, California.
- Siniff, D. B., and K. Ralls. 1991. Reproduction, survival and tag loss in California sea otters. *Marine Mammal Science* 7:211-229.
- Thomas, C. D., and W. E. Kunin. 1999. The spatial structure of populations. *Journal of Animal Ecology* 68:647-657.
- USFWS. 2003. Final revised recovery plan for the southern sea otter (*Enhydra lutris nereis*). U.S. Fish and Wildlife Service. Portland, OR.
- Virgl, J. A., and F. Messier. 2000. Assessment of source-sink theory for predicting demographic rates among habitats that exhibit temporal changes in quality. *Canadian Journal of Zoology* 78:1483-1493.
- Watt, J., D. B. Siniff, and J. A. Estes. 2000. Inter-decadal patterns of population and dietary change in sea otters at Amchitka Island, Alaska. *Oecologia* 124:289-298.

Tables

Table 1. Parameter estimates used for the simulation model. Numbers in parentheses (following mean values) are standard errors, while two numbers separated by a hyphen indicate the range of values used in simulation runs.

Model Parameter	Juveniles	Sub-adults	Adults	Aged Adults
Annual birth rates	0	0.4	0.98	0.9
Wean success rates	0	0.4 (0.10)	0.061 (0.07)	0.8 (0.07)
<u>Female annual survival rates</u>				
Estimates 1-10: see Ch. 2, Appendix B				
sub-populations 1-2	0.838 - 0.858	0.847 - 0.869	0.843 - 0.870	0.509 - 0.556
sub-population 3	0.833 - 0.853	0.842 - 0.864	0.836 - 0.866	0.504 - 0.550
sub-population 4	0.847 - 0.867	0.854 - 0.876	0.847 - 0.874	0.505 - 0.554
sub-populations 5-6	0.848 - 0.869	0.856 - 0.878	0.849 - 0.876	0.508 - 0.557
Estimate 11: 2001-2003 ¹				
sub-populations 1-2, 5-6	0.85 (0.145)	0.88 (0.145)	0.91 (0.088)	0.55 (n/a)
sub-populations 3-4	0.84 (0.060)	0.84 (0.060)	0.84 (0.060)	0.55 (n/a)
Estimate 12: 1980's, all sub populations	0.85 (0.145)	0.88 (0.145)	0.91 (0.088)	0.55 (n/a)
<u>Male annual survival rates</u>				
Estimates 1-10: see Ch. 2, Appendix B				
sub-populations 1-2	0.782 - 0.809	0.782 - 0.811	0.746 - 0.784	0.328 - 0.371
sub-population 3	0.776 - 0.802	0.776 - 0.805	0.739 - 0.778	0.322 - 0.365
sub-population 4	0.793 - 0.820	0.791 - 0.821	0.751 - 0.791	0.324 - 0.370
sub-populations 5-6	0.795 - 0.822	0.794 - 0.823	0.754 - 0.793	0.327 - 0.373
Estimate 11: 2001-2003 ¹				
sub-populations 1-2, 5-6	0.88 (0.179)	0.88 (0.179)	0.87 (0.095)	0.35 (n/a)
sub-populations 3-4	0.88 (0.179)	0.88 (0.179)	0.84 (0.060)	0.35 (n/a)
Estimate 12: 1980's, all sub populations	0.88 (0.179)	0.88 (0.179)	0.70 (0.167)	0.35 (n/a)
<u>Laplace Dispersal Parameters (σ) ²</u>				
Females, all sub-populations	32.6 - 83.1	32.6 - 83.1	7.5 - 11.7	7.5 - 11.7
Males, sub-population 1-3	63.2 - 171.0	63.2 - 171.0	7.6 - 20.6	7.6 - 20.6
Males, sub-population 4	63.2 - 171.0	63.2 - 171.0	39.5 - 95.9	39.5 - 95.9
Males, sub-populations 5-6	63.2 - 171.0	63.2 - 171.0	79.7 - 150.0	79.7 - 150.0

¹ Estimates correspond to 1980-'s values for locations or stages not measured in 2001-2003

² Units = 500m increments (ATOS values)

Table 2. Summary of results from simulations

Variable	Mean	Std. dev.	Median	Mode	L95	U95
Net rate of increase (λ)	1.011	0.021	1.012	1.01	0.971	1.052
S. of Pt. Conception, 10yrs	120.69	38.477	117	107	57	207
S. of Pt. Conception, 15yrs	136.63	53.212	131	121	53	259
Southern Exp. Speed(km/yr)	5.0679	3.3469	4.86	1.43	0.422	13.82
Range End, 10 yrs	1271		1267	1199	1178	1446
Range End, 15 yrs	1322		1316	1213	1183	1584

Figure Captions

Figure 1. Map of central California showing current range of the southern sea otter (excluding San Nicolas Island), and identifying the spatial arrangement of the six sub-populations identified for the simulation model.

Figure 2. The spatial distribution of sea otters along the coast (on a north-to-south axis) is plotted as a histogram for each of the six sub-populations (see Figure 1), based on the results of the five most recent spring surveys. *Beta* probability density functions were fit to each data set and are overlain on the histograms: the parameter values for each function are displayed above each curve. The *Beta* functions were used in the calculation of movement rates between sub-populations (see text).

Figure 3. Annual dispersal distance frequency histograms are shown for adult females (pink bars) and juvenile females (blue bars). Laplace probability functions were fit to each of these distributions (dashed and solid lines), and used in the calculation of stage-specific movement rates. Note that the distribution for juvenile females shows greater dispersion, which is reflected by a higher value of the scale parameter σ . Similar functions were calculated for males (not shown here).

Figure 4. Results of a historical simulation of population dynamics for the southern sea otter population over the years 1989–2003. Predicted population counts, based on the simulation, are shown at top, with observed counts for comparison. Predicted range expansion to the south (increasing ATOS values over time) is shown at bottom, with observed range-end boundaries shown for comparison. The range end was defined as the point along the coast at which 99.75% of the sea otter population was to the north, based on the annual spring survey. A linear least-squares curve was fit to the observed range-end dataset, and is plotted (along with the 95% prediction interval) to illustrate the correspondence between the predicted and observed mean rate of expansion.

Figure 5. A frequency distribution of predicted outcomes is shown for two of the key simulation results: the expected number of independent sea otters south of Pt. Conception after 10 years (top) and after 15 years (bottom). The distributions were well described by negative-binomial probability distributions.

Figure 6. A frequency distribution of the predicted rate of southward range expansion is shown, based on the results of 10,000 replicate simulations. A weibull probability distribution was fit to the raw data.

Figure 7. Results of a sensitivity analysis, showing the relative proportion of the variance in simulation dynamics explained by three groups of model parameters: dispersal rates, survival rates at the south of the range (sub-populations 5 and 6) and survival rates at the center of the range (sub-populations 3 and 4). Sensitivities are shown for three response variables: A) the number of individual otters south of pt. conception after 15 years, B) average southward wave speed, or rate of range expansion to the south, and C) the overall rate of population increase over the simulation period.

Figure 8. Results of a sensitivity analysis of dispersal parameters, showing the relative proportion of the variance in simulation dynamics explained by stage- and sex-specific dispersal rates. Sensitivities are shown for two response variables: A) the number of individual otters south of pt. conception after 15 years, B) average southward wave speed, or rate of range expansion to the south.

Figure 9. Results of a sensitivity analysis of survival parameters, showing the relative proportion of the variance in simulation dynamics explained by stage- and sex-specific survival rates. Sensitivities are shown for three response variables: A) the number of individual otters south of pt. conception after 15 years, B) average southward wave speed, or rate of range expansion to the south, and C) the overall rate of population increase over the simulation period.

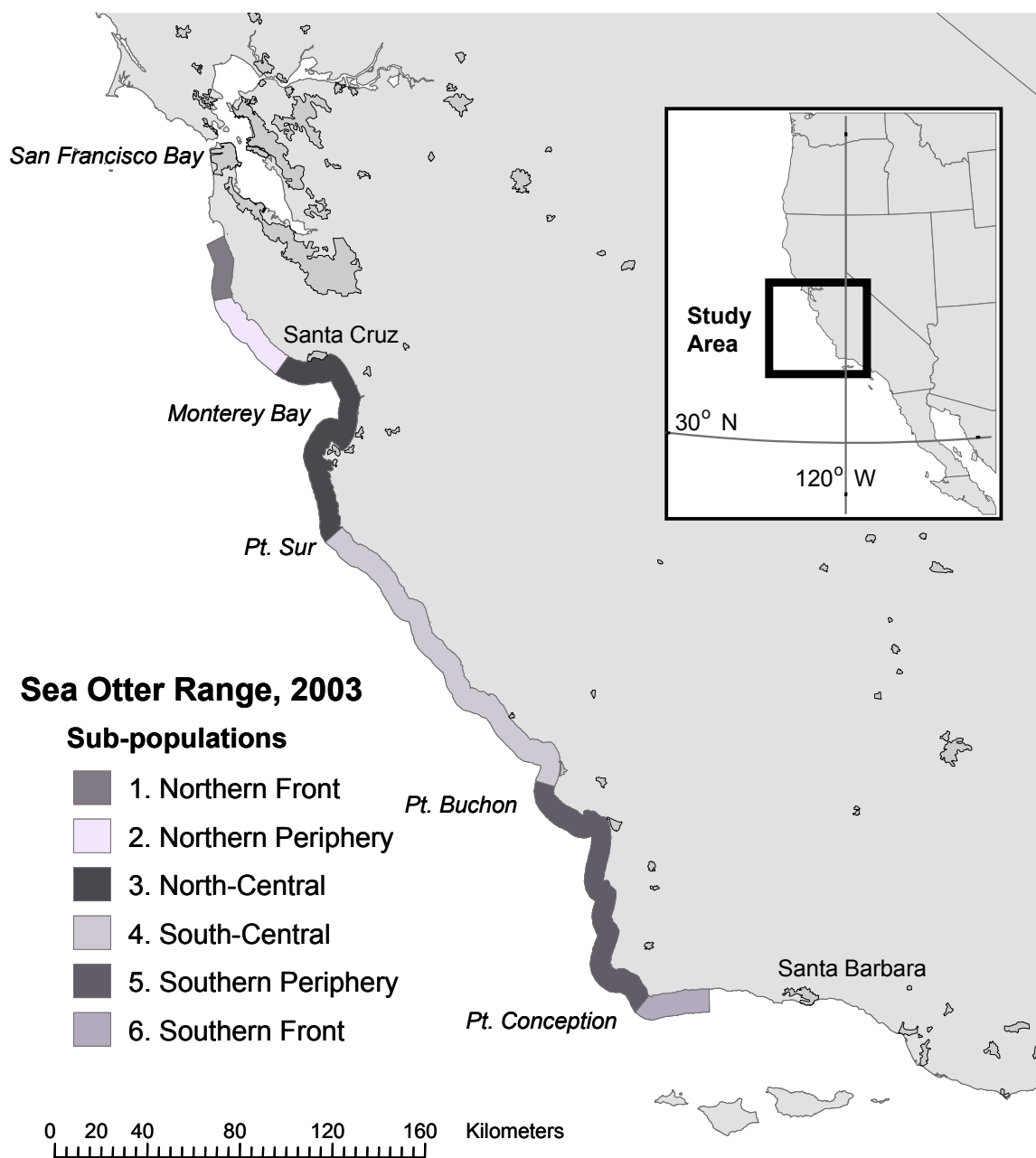


Figure 1

Relative density of sea otters (1999-2003 spring surveys)

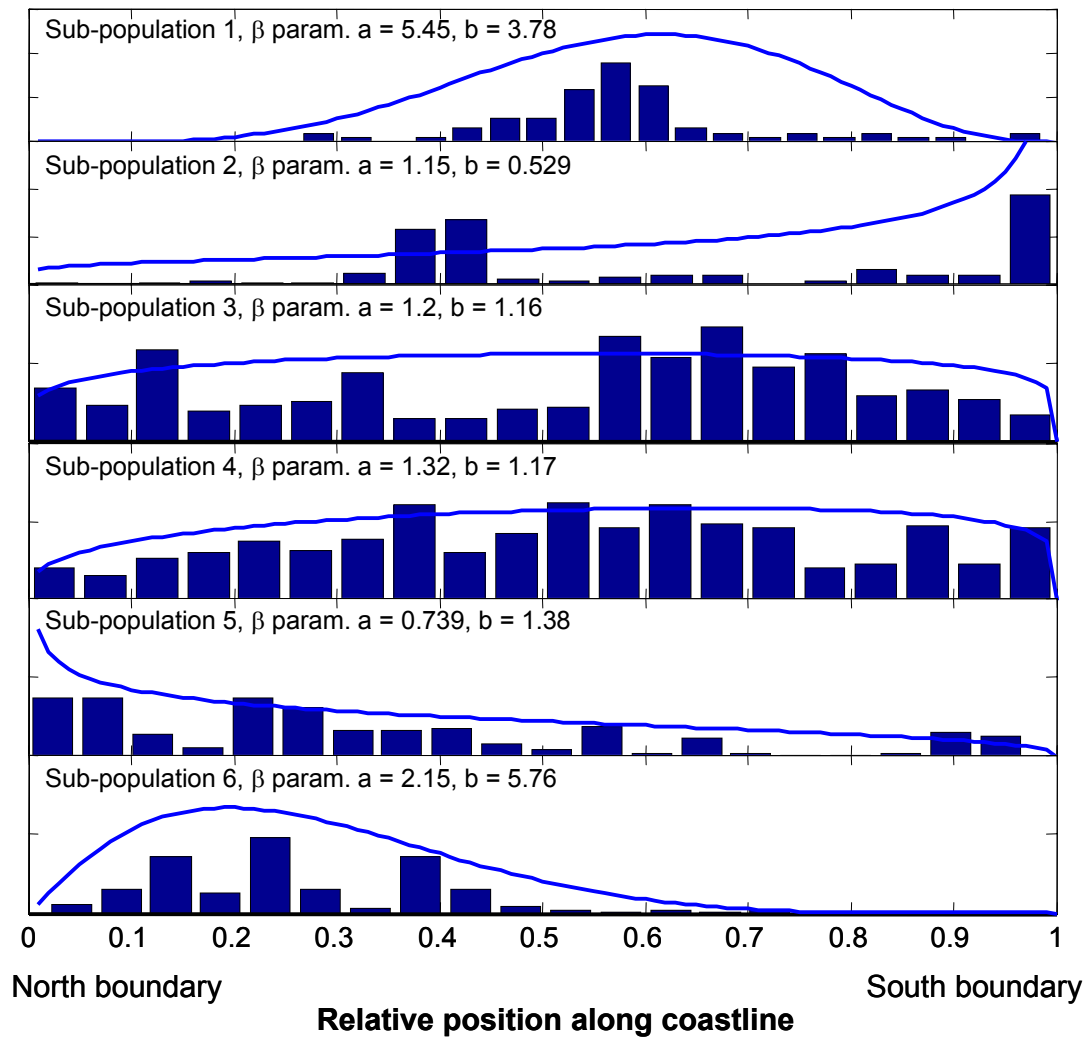


Figure 2

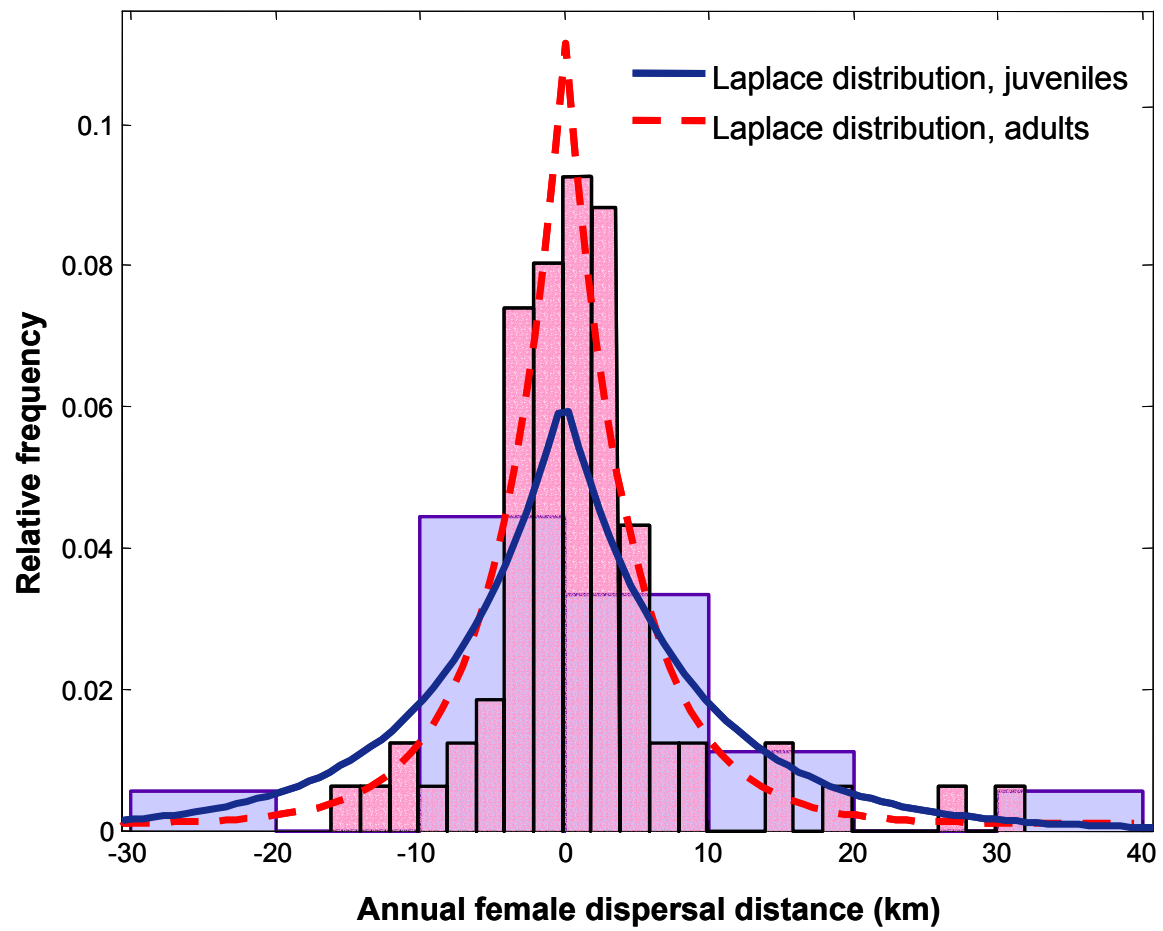


Figure 3

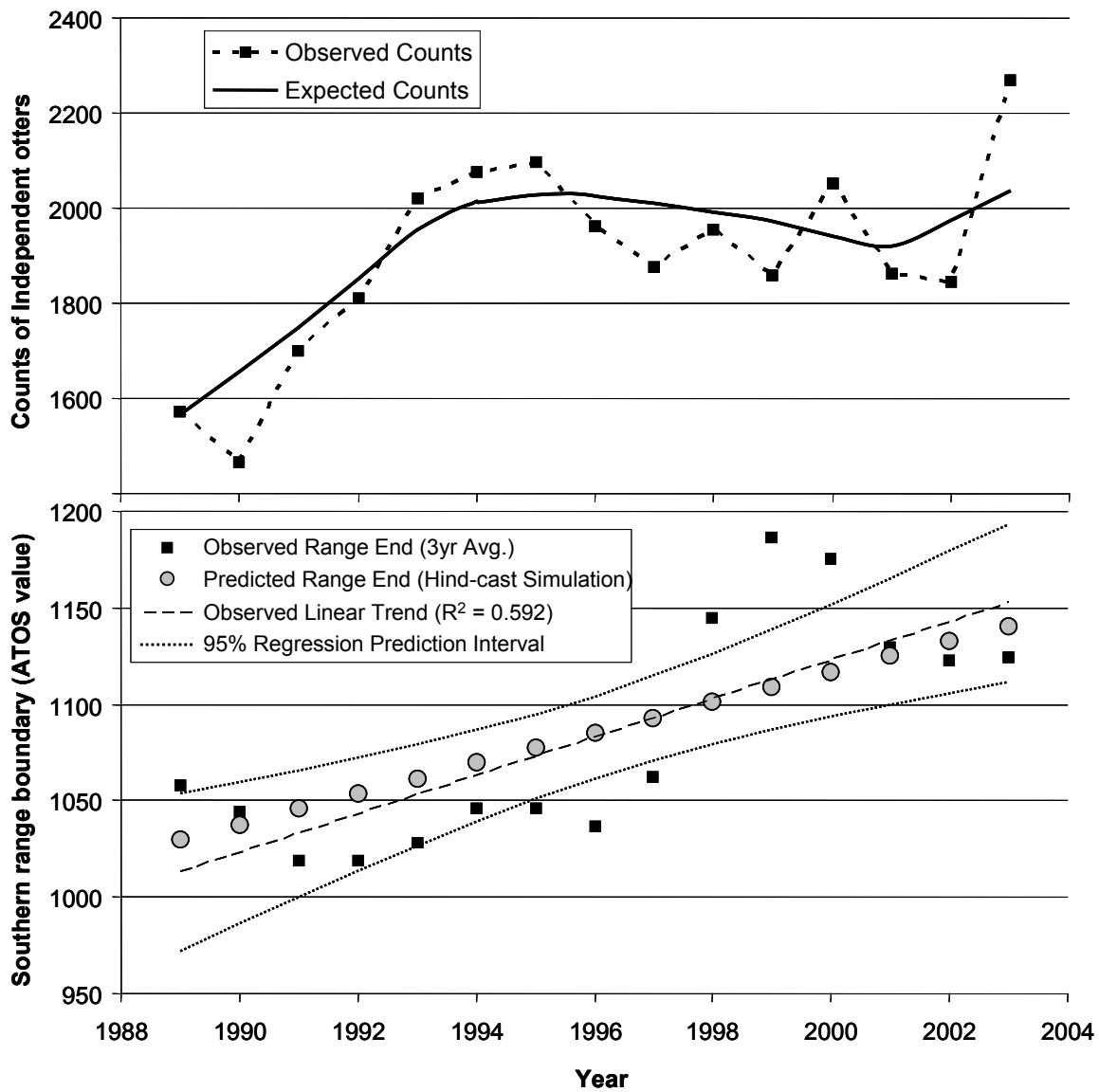


Figure 4

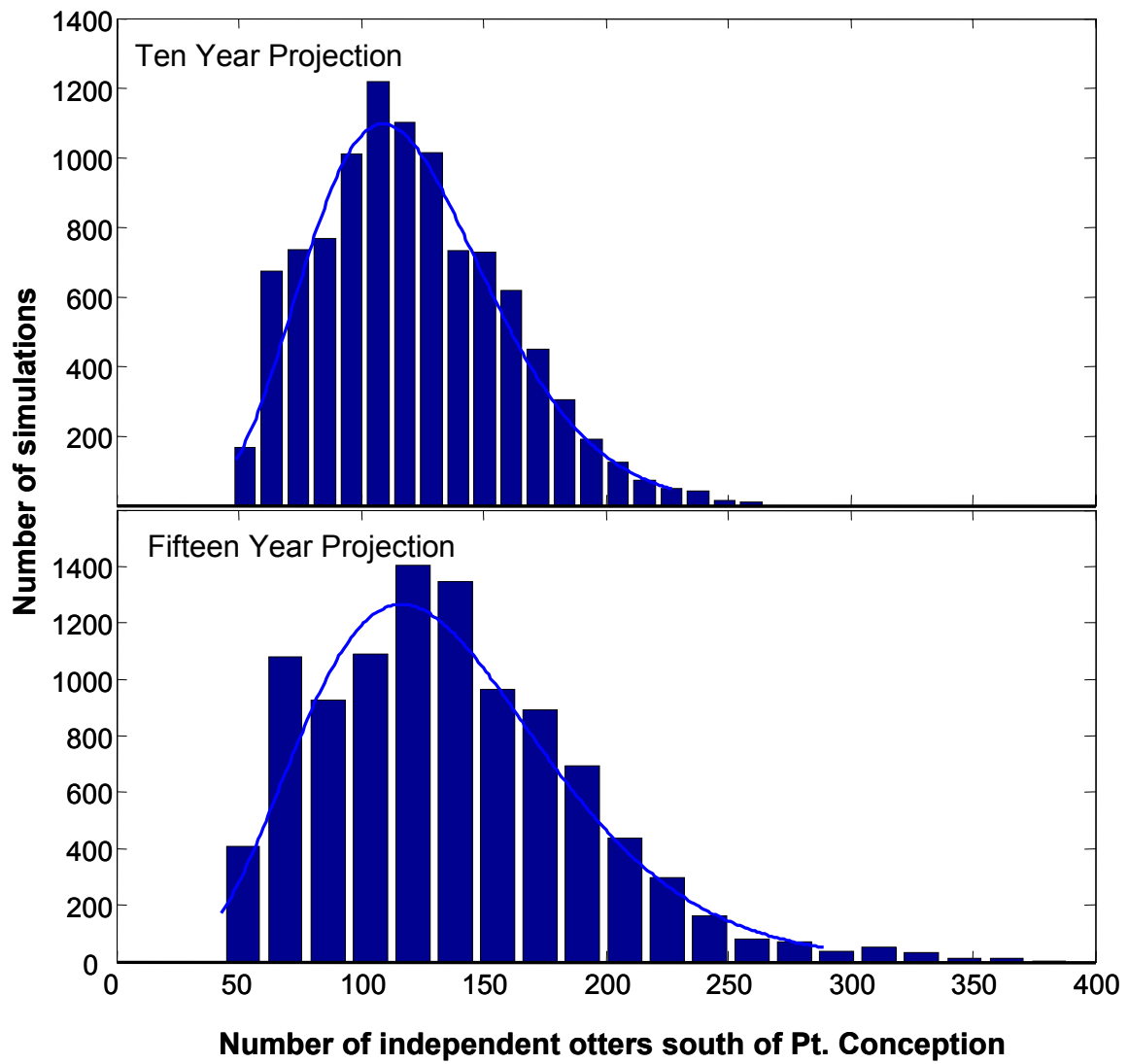


Figure 5

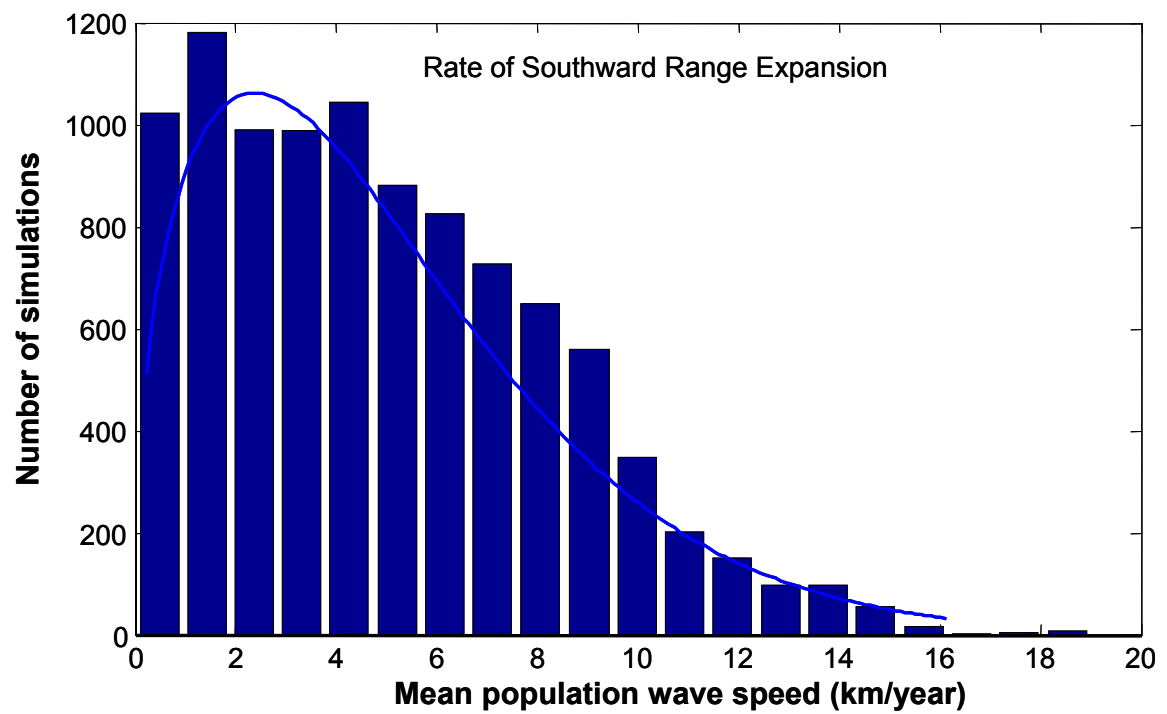


Figure 6

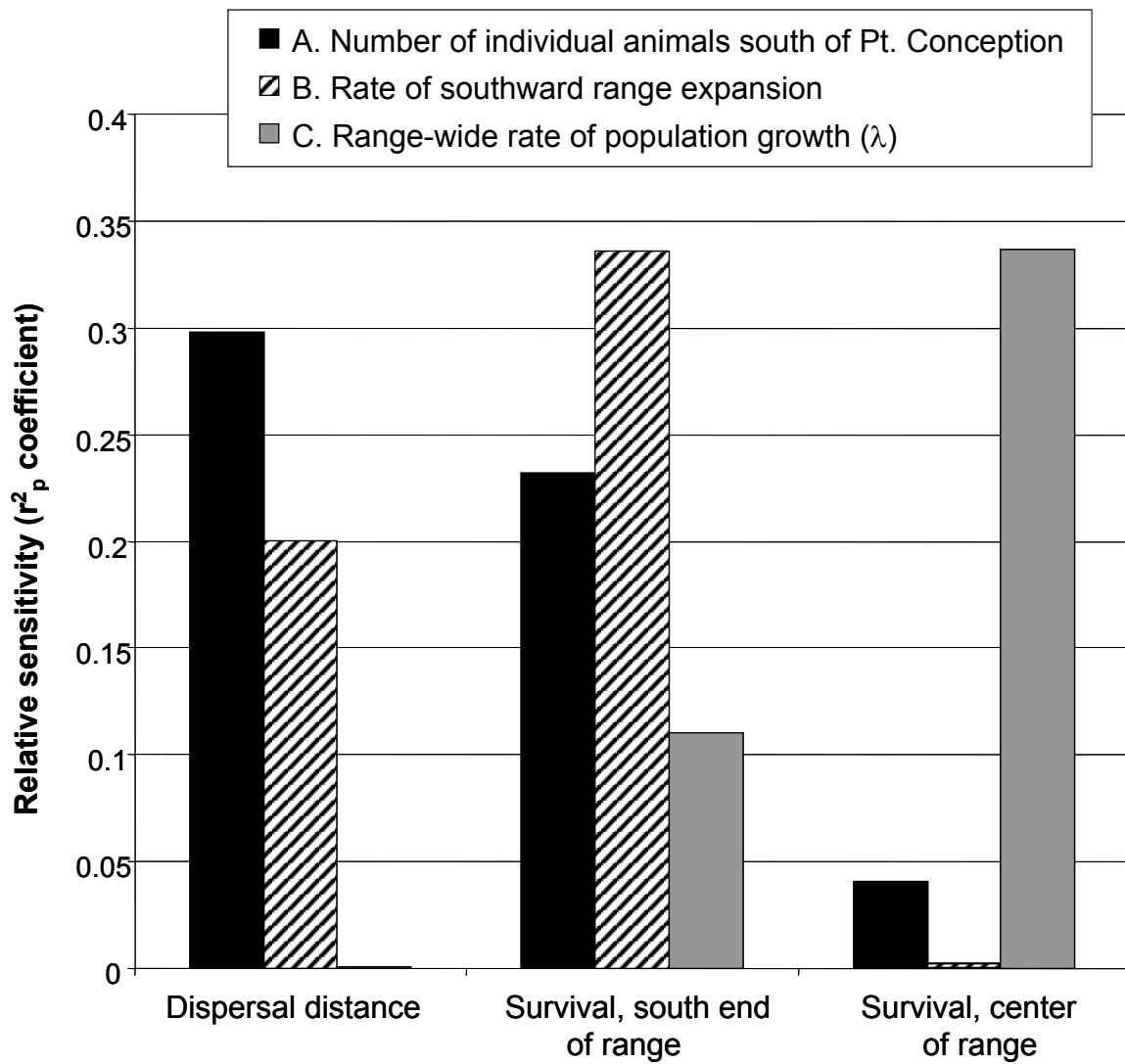


Figure 7

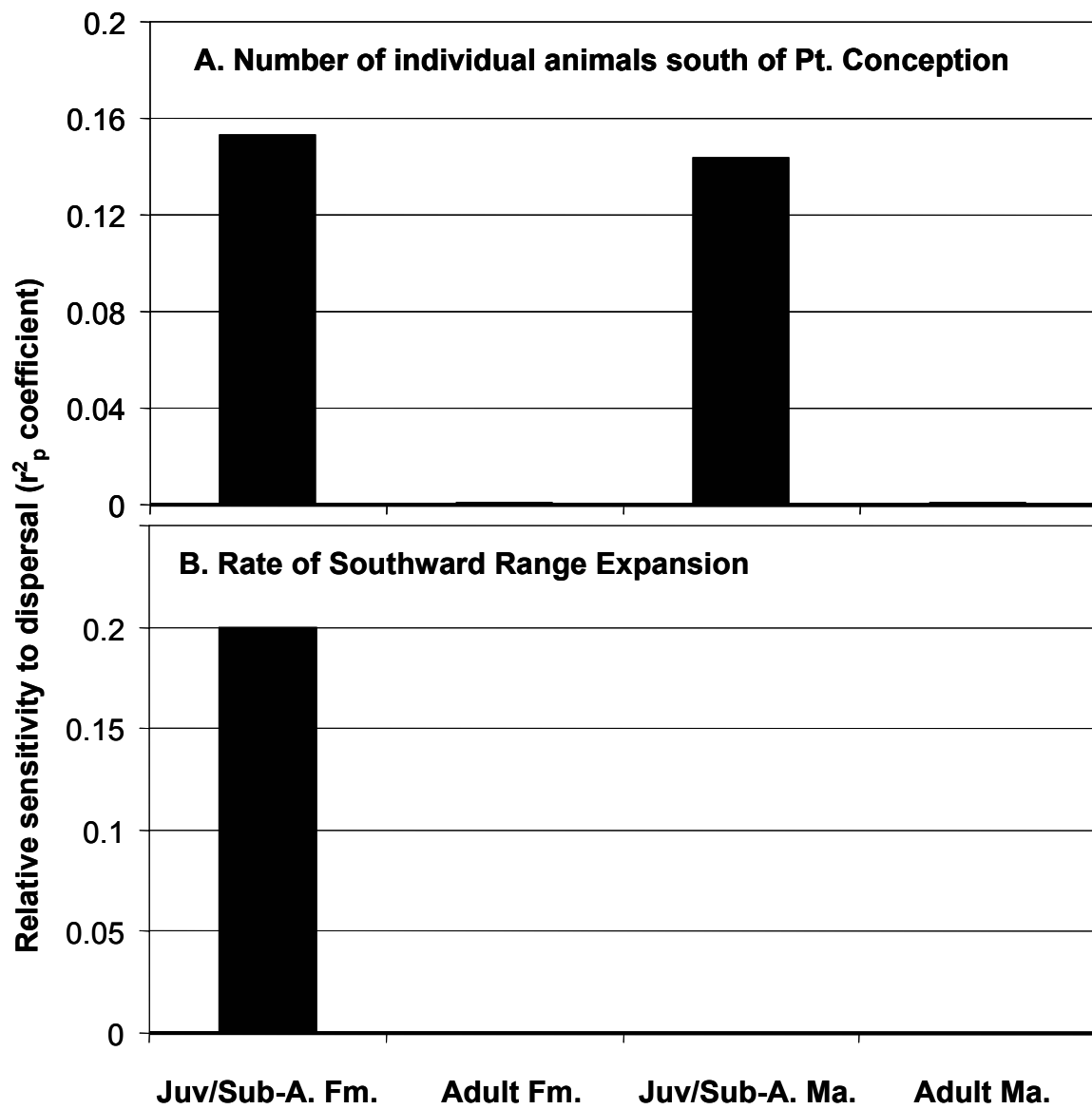


Figure 8

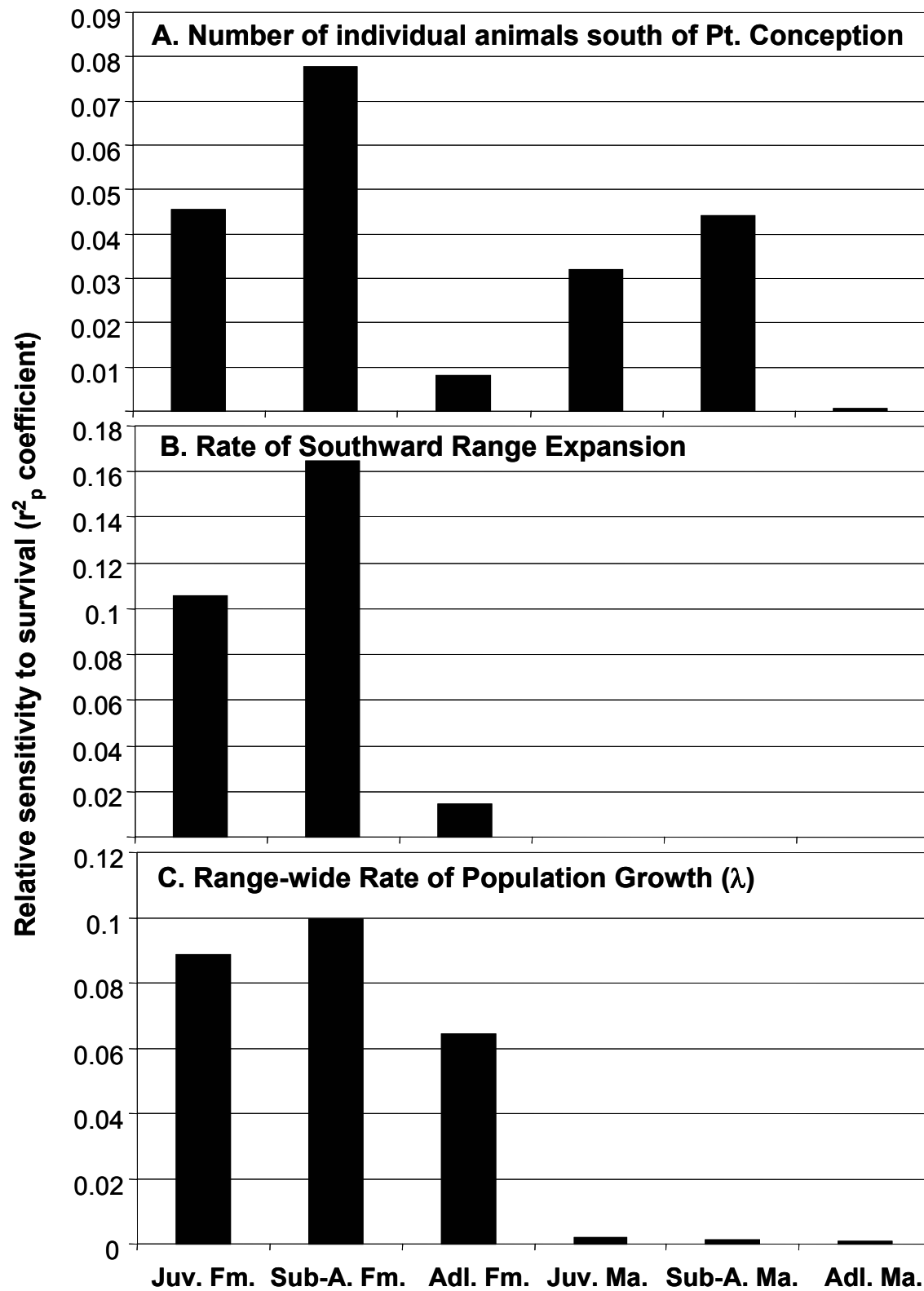


Figure 9